Symmetry Breaking with the SCAN Density Functional Describes Strong Correlation in the Singlet Carbon Dimer

John P. Perdew[a,b,*], Shah Tanvir ur Rahman Chowdhury[c], Chandra Shahi[a], Aaron D. Kaplan[a], Duo Song[d], and Eric J. Bylaska[d]

[a]Department of Physics, Temple University, Philadelphia, PA 19122

[b]Department of Chemistry, Temple University, Philadelphia, PA 19122

[c]Thayer School of Engineering, Dartmouth College, Hanover, NH 03755

[d]Pacific Northwest National Laboratory, Richland, WA 99353

Abstract: The SCAN (strongly constrained and appropriately normed) meta-generalized gradient approximation (meta-GGA), which satisfies all 17 exact constraints that a meta-GGA can satisfy, accurately describes equilibrium bonds that are normally correlated. With symmetry breaking, it also accurately describes some *sd* equilibrium bonds that are strongly correlated. While *sp* equilibrium bonds are nearly always normally correlated, the C_2 singlet ground state is known from correlated wave-function theory to be a rare case of strong correlation in an *sp* equilibrium bond. Earlier work that calculated atomization energies of the molecular sequence B_2, C_2, O_2, and F_2 in the local spin density approximation (LSDA), the Perdew-Burke-Ernzerhof (PBE) GGA, and the SCAN meta-GGA, without symmetry breaking in the molecule, found that only SCAN was accurate enough to reveal an anomalous under-binding for C_2. This work shows that spin symmetry breaking in singlet C_2, the appearance of net up- and down-spin densities on opposite sides (not ends) of the bond, corrects that under-binding, with a small SCAN atomization-energy error more like that of the other three molecules, suggesting that symmetry-breaking with an advanced density functional might reliably describe strong correlation. This article also discusses some general aspects of symmetry breaking, and the insights into strong correlation that symmetry-breaking can bring.

*Corresponding author: perdew@temple.edu, 1-215-204-1407

Introduction

The spin-density functional theory of Kohn and Sham[1,2] is an exact in principle self-consistent-field formalism for the ground-state energy and spin densities of a system of interacting non-relativistic electrons in the presence of an external possibly-spin-dependent potential $v_\sigma(\boldsymbol{r})$. In practice, only the exchange-correlation energy as a functional of the spin densities must be approximated. The computationally-efficient approximations on the first three rungs of Jacob's Ladder[3] are single integrals of the form

$$E_{xc}^{approx}[n_\uparrow, n_\downarrow] = \int d^3 \, rn\varepsilon_{xc}^{approx}(n_\uparrow, n_\downarrow, \nabla n_\uparrow, \nabla n_\downarrow, \tau_\uparrow, \tau_\downarrow). \qquad (1)$$

Here $n(\boldsymbol{r}) = n_\uparrow(\boldsymbol{r}) + n_\downarrow(\boldsymbol{r}) = \sum_{i\sigma}^{occup} |\psi_{i\sigma}(\boldsymbol{r})|^2$ is the total electron density, and

$$\tau_\sigma(r) = \sum_i^{occup} \frac{1}{2} \, |\nabla\psi_{i\sigma}(\boldsymbol{r})|^2 \qquad (2)$$

is the positive orbital kinetic energy density. Rung 1 of the ladder (e.g., LSDA[1,2.4]) uses only the local spin densities, rung 2 (e.g., PBE[5] GGA) adds the gradients of the spin densities, and rung 3 (e.g., SCAN[6] or r²SCAN[7] meta-GGA) adds the kinetic energy densities.

There is a nearly straight line[8] from the exact density functional theory to its first-principles approximations (e.g., LSDA, PBE, or SCAN), which proceeds from exact (if impractical) expressions for $E_{xc}[n_\uparrow, n_\downarrow]$ to the derivation of mathematical properties of the exact functional that can be satisfied by an approximation on a given rung, and finally to imposing those constraints on the approximate functional. Appropriate norms, or systems in which a given rung can be accurate for the exchange energy alone and the correlation energy alone, can be safely fitted. Appropriate norms for all three rungs include electron gases of uniform spin densities. Appropriate norms for rung 3 include closed-subshell atoms. LSDA inherits 8 exact constraints from its uniform gas norm, PBE satisfies 11 exact constraints appropriate to the GGA level, and SCAN satisfies all 17 known exact constraints that a meta-GGA can satisfy. The energies of molecules and solids, often fitted by empirical functionals, are not appropriate norms, because of an understood but imperfect and uncontrolled cancellation between errors in the approximate exchange and correlation energies. While empirical functionals interpolate between bonds, first-principles approximations predict[9] them, typically working better than empirical functionals for artificial molecules that are unlike those commonly fitted.

SCAN with a long-range van der Waals correction was more accurate than other tested functionals from the first three rungs, and more accurate than some hybrid functionals employing a fraction of exact exchange, in a 2017 test[10] on the GMTKN55 suite of 55 molecular test sets. SCAN is also accurate for insulating solids. For some strongly-correlated sd-bound solids, such as the cuprates[11] and manganese dioxides[12], symmetry-broken SCAN is accurate without a "Hubbard-like:"$+U$ correction (sometimes interpreted as a self-interaction correction[13]). In other strongly-correlated transition-metal oxides, symmetry-broken SCAN requires a $+U$ correction, but one significantly smaller than PBE requires[14]. Range-separated GGA hybrid functionals with short-range exact exchange can describe[15] many strongly-correlated solids better than LSDA or GGA and without a material-dependent parameter like U. Such functionals[16] and other nonlocal functionals[17] can also describe polaronic symmetry breaking.

For equilibrium bonds, a self-interaction correction seems to be much more needed for sd than for sp bonds. The Perdew-Zunger self-interaction correction[18] is first-principles, but is not reliably accurate due to the lobedness of its localized one-electron densities[19]. Perhaps in the future an improved self-interaction correction to a SCAN-like functional will lead to a reliable and widely-useful description of strong correlation via symmetry breaking. For now, any strongly-correlated equilibrium sp bond is of special interest as a test of the ability of symmetry breaking to describe strong correlation. Such bonds are rare, but the singlet ground state of the molecule C_2 is known to be strongly correlated. This molecule has an avoided crossing of two energy surfaces near its equilibrium bond length, and has been studied carefully with the full configuration interaction quantum Monte Carlo (FCIQMC) correlated-wavefunction approach.[20]

Symmetry breaking (in both wavefunction and density functional theories) and strong correlation have attracted the interest of many, notably Gustavo E. Scuseria and Richard L. Martin[15,22,23]. Strong correlation arises when degenerate or nearly degenerate Slater determinants are strongly mixed by the electron-electron pair interaction. This leads to correlation or exchange-correlation energies more negative than those that a standard approximate density functional can produce. A standard approximate functional places the total energy of a strongly-correlated state too high, and can often lower its energy by breaking a symmetry. Breaking the symmetry can break the degeneracy and return the system to a normally-correlated state whose energy the approximate functional can properly describe. An alternative rationale[24] for spin-symmetry breaking re-interprets approximate spin-density

functional calculations as approximations to a nearly-exact theory for total energy, total electron density, and on-top pair density.

The importance of symmetry breaking was recognized[25] early in the history of density functional theory: For the singlet H_2 molecule at its equilibrium bond length, standard approximate functionals can be accurate for the energy. As the bond length is stretched toward infinity, preserving the correct singlet (hence spin-unpolarized) ground state requires a strongly negative correlation energy which the approximate functional cannot provide. In correlated-wavefunction language, the singlet ungerade excited state is dropping toward and becoming degenerate with the singlet gerade ground state. At a critical Coulson-Fischer bond length, the approximate functional starts to produce a spin-polarized (hence symmetry-broken) self-consistent density, which is needed for a realistic H_2 binding energy curve. As the bond length tends to infinity, one recovers an up-spin H atom on one end of the bond and a down-spin H atom on the other, which is actually correct in the sense that such a spin-density fluctuation freezes out, not on an infinite time scale but on a macroscopic one. Thus the symmetry-breaking provides a physical picture of the strong correlation present at large bond length. In this limit, the symmetry breaking has converted a strong correlation energy into zero correlation energy (literally zero in SCAN, which is self-correlation free).

For a given Hamiltonian, eigenstates of a complete set of commuting observables (including symmetry operators that leave the Hamiltonian invariant) can always be found. In this sense, symmetry breaking is not required in exact wavefunction and density functional theories. Approximate density functionals that avoid symmetry breaking have also been constructed[26,27]. Still, as pointed out in the previous paragraph, symmetry breaking is sometimes fully real and perhaps more often revealing.

An interesting recent comment by Alex Zunger[28] suggests that all or at least many "quantum materials" (exotic extended systems, including strongly-correlated ones) can be well described by full symmetry breaking with standard approximate functionals (including in some cases $+U$-style self-interaction corrections). Much is known about symmetry breaking[29,30], but much remains to be determined, including its reliability for the description of strong correlation with advanced constraint-based density functionals.

Open-shell atoms like B, C, O, and F have degenerate ground states that can be either symmetry-preserving or symmetry-breaking. LSDA, PBE, and SCAN

appear not to make significant differences in energy between them. *sp* atoms do not seem to exhibit strong correlation, although bonded systems can do so. The molecules B_2, C_2, O_2, and F_2 have closed-subshell non-degenerate ground states, A recent study[31] of the atomization energies of B_2, C_2, O_2, and F_2 used symmetry-unbroken solutions for the molecules (Fig.1 of Ref. 31). The mean absolute errors for B_2, O_2, and F_2 were 1.7 eV in LSDA, 0.7 eV for PBE, and 0.1 eV for SCAN. The errors of LSDA and PBE were too large to permit the identification of singlet C_2 as the only strongly-correlated molecule in this set. But the much smaller errors of SCAN showed that singlet C_2 is strongly and uniquely under-bound (by 1.5 eV) in symmetry-unbroken SCAN. We will show here that this under-binding is corrected, and the error becomes similar to the errors for the other three molecules, within symmetry-broken SCAN. Thus we will show that the strong correlation in singlet C_2, which is far more subtle than that in highly-stretched H_2, can be captured by symmetry-broken SCAN.

Computational Details

The calculations in this study were performed with the pseudopotential plane-wave NWPW[32] module implemented in the NWChem[33,34] software package. The web application EMSL Arrows[35] was used to set up and perform all the calculations. The LSDA[1,2] (in the parametrization of Ref. 4), PBE GGA[5] and SCAN meta-GGA[6] were employed to account for the exchange and correlation energy. In our plane-wave calculations, the valence electron interactions with the atomic core for carbon were approximated with generalized norm-conserving Hamann[36] pseudopotentials modified to the separable form suggested by Kleinman and Bylander[37]. The pseudopotentials used in this study were constructed with the following core radii: $r_{cs} = 0.800$ bohr, $r_{cp} = 0.850$ bohr and $r_{cd} = 0.850$ bohr. The electronic wavefunctions were expanded using a plane-wave basis in a simple cubic box of $L = 26$ bohr with a wavefunction cutoff energy of 100 Ry and a density cutoff energy of 200 Ry.

Both restricted and unrestricted calculations with aperiodic free space boundary conditions[38,39] were performed for the singlet electronic state of C_2. The spin-symmetry breaking was "nudged". For the unrestricted calculations, the initial Kohn-Sham molecular orbitals were randomly generated with numerical noise to break the spin-symmetry. This is automatically done by default in NWChem.

Results and Discussion

Table I presents our calculated atomization energies for the strongly-correlated singlet state of the carbon dimer. The results without spin-symmetry breaking in the molecule show a familiar pattern in which the atomization energy is strongly reduced from LSDA to PBE GGA to SCAN meta-GGA. The atomization energy with spin-symmetry breaking is also reduced in the same order, but much less strongly. The error for symmetry-broken SCAN is 0.0 eV, in line with the 0.1 eV mean absolute error of SCAN for the normally-correlated and hence symmetry-unbroken dimers B_2, O_2, and F_2 discussed in the Introduction and in Ref. 31. Molecular spin-symmetry breaking in SCAN increases the atomization energy by 1.4 eV.

The last column or "difference" in Table I is the energy lowering due to the appearance of non-zero net spin density in a singlet state that in a symmetry-preserving theory would have zero net spin density everywhere. This difference increases strongly from 0.3 eV for LSDA to 0.7 eV for PBE GGA to 1.4 eV for SCAN meta-GGA. Compare Table I of Ref. 31, in which the energy difference between spherical and non-spherical density for open-subshell B, C, O, and F atoms also increases strongly from LSDA to PBE GGA to SCAN. Added ingredients in Eq. (1) can make an approximate functional much more sensitive to the density[31], at least in some cases.

Figures 1, 2, and 3 show the calculated binding energy curves for singlet C_2 in LSDA, PBE GGA, and SCAN, respectively. The Coulson-Fischer point always occurs at a bond length much shorter than the equilibrium bond length (~ 1.25 Å for all three functionals, with or without symmetry breaking). The pattern of spin-symmetry breaking, as shown in these figures, is also similar for all three functionals, with up and down spin densities appearing on opposite sides (not opposite ends as in stretched H_2) of the bond (double in C_2 but single in H_2). The earliest spin-symmetry-broken solution in singlet C_2 was end-to-end[40]. A side-to-side alternation of lower energy was found in Ref. 41 with the PW91 GGA (which preceded but is numerically similar to the PBE GGA). We suspect that the symmetry breaking is revealing low-frequency spin-density fluctuations that contribute to the strong correlation in C_2.

The symmetry-unbroken singlet wavefunction of C_2 would have the total-spin quantum number $S = 0$ and thus $\langle \hat{S}^2 \rangle = S(S+1) = 0$. Symmetry breaking of the Kohn-Sham non-interacting wavefunction increases from LSDA ($\langle \hat{S}^2 \rangle = 0.66$) to PBE GGA ($\langle \hat{S}^2 \rangle = 0.89$) to SCAN meta-GGA ($\langle \hat{S}^2 \rangle = 1.07$).

The calculated Kohn-Sham orbitals explain the complicated pattern of net spin density shown in the insets of Figs. 1-3. The net bonding in C_2 arises from four electrons in the higher-energy occupied molecular orbitals. In the symmetry-unbroken molecule, these are two degenerate π bonding orbitals. In the symmetry-broken molecule, these are a highest-occupied σ orbital that is the same for spin-up and spin-down, and two next-highest-occupied banana bonds, one for spin down with its banana lobe above the bond axis and one for spin up with its banana lobe below in the page of each figure. A larger banana lobe on one side of the bond axis is accompanied by a smaller and more compact lobe of the same orbital on the other side. The net spin density has an integrated net down (blue) spin density above the bond axis and an integrated net up (orange) spin density below the bond axis, as shown in the figures. The integral of the difference in spin-up and spin-down densities (net number of spin-up electrons) is 0.35 (-0.35) from unrestricted LSDA, 0.44 (-0.44) from unrestricted PBE GGA and 0.63 (-0.63) from unrestricted SCAN meta-GGA below (above) the bond axis in Figs. 1-3.

In summary, spin-symmetry breaking with the SCAN meta-GGA captures the energetics (and perhaps also the modality) of strong correlation in the singlet carbon dimer at its equilibrium geometry. Allowing for the possibility of symmetry breaking, SCAN provides an accurate description of the dimer sequence B_2, C_2, N_2, and O_2, in which only C_2 is strongly correlated. For these equilibrium sp bonds, no need for a self-interaction correction is expected. When a self-interaction correction to the SCAN-like functionals is perfected, symmetry breaking might provide a widely reliable description of strong correlation in molecules and solids.

Symmetry-broken states of finite systems may be "static or strong correlation" states that persist for a long-time (long enough to have well-defined energies), if not forever[29,30]. Reliable access to such states is through the dynamic structure factor[25,42] or spectral function[29,30] describing the dynamic correlations that are hidden within a time-independent wavefunction, that are revealed in the expectation values of relevant time-dependent operators, and that are in fact responsible for the exchange-correlation energy that is approximated in ground-state density-functional theory.

References

1. Kohn W, Sham LJ. 1965. Self-consistent equations including exchange and correlation. *Phys. Rev.* 140:A1133
2. von Barth U, Hedin L. 1972. A local exchange-correlation potential for the spin-polarized case.1. *J. Phys. C* 5:1629-1642
3. Perdew J, Schmidt K. 2001. Jacob's ladder of density functional approximations for the exchange-correlation energy, *AIP Conf. Proc.* 577(1):1-20
4. Perdew JP, Wang Y. 1992. Accurate and simple analytic representation of the electron-gas correlation energy. *Phys. Rev.* B 81(8):1200-1211
5. Perdew JP, Burke K, Ernzerhof M. 1996. Generalized gradient approximation made simple. *Phys. Rev. Lett.* 77:3865
6. Sun J, Ruzsinszky A, Perdew JP. 2015. Strongly constrained and appropriately normed semilocal density functional. *Phys. Rev. Lett.* 115:036402
7. Furness JW, Kaplan AD, Ning J, Perdew JP, Sun J. 2020. Accurate and numerically efficient r^2SCAN meta-generalized gradient approximation. *J. Phys. Chem. Lett.* 11(19):8208-8215. Erratum, *ibid.* 2020. 11:9248.

8. Perdew JP. 2023. Modern density functionals derived from first principles. Invited article for "Advanced Electronic Structure Methods", section editor Krishnan Raghavachari, in *Comprehensive Computational Chemistry* (Elsevier)

9. Kaplan AD, Levy M, Perdew JP. 2023. Predictive power of the exact constraints and appropriate norms in density-functional theory. Invited review in *Ann. Rev. Phys. Chem.*

10. Goerigk L, Hansen A, Bauer C, Ehrlich S, Najibi A, Grimme S. 2017. A look at the density functional zoo with the advanced GMTKN55 database for general main group thermochemistry, kinetics, and noncovalent interactions. *Phys. Chem. Chem. Phys*. 19:32184-32215

11. Zhang Y, Lane C, Furness JW, Barbiellini B, Perdew JP, Markiewicz RS. Bansil A, Sun J. 2020. Competing stripe and magnetic phases in the cuprates from first principles. *Proc. Nat. Acad. Sci.* USA 117(1):68-72

12. Kitchaev DA, Peng H, Liu Y, Sun J, Perdew JP, Ceder G. 2016. Energetics of MnO_2 polymorphs in density functional theory. *Phys. Rev. B* 93:045132

13. Cococcioni M, de Gironcoli S, 2005. Linear response approach to the calculation of the effective interaction parameters in the LDA+U method. *Phys. Rev. B* 71:03510

14. Gautam GS, Carter EA. 2018. Evaluating transition metal oxides within DFT-SCAN and SCAN+U. *Phys. Rev. Mater.* 2(9):095401

15. Wen XD, Martin RL, Henderson TM, Scuseria GE. 2013. Density functional theory studies of the electronic structure of solid-state actinide oxides. *Chem. Rev.*113:1063-1096

16. Peng H, McKendry IG, Ding R, Thenuwara AC, Kang Q, Shumlas SL, Strongin DR, Zdilla MJ, Perdew JP. 2017. Redox properties of birnessite from a defect perspective. *Proc. Nat. Acad. Sci. USA* 114(36): 9523-9524

17. Falletta S, Pasquarello A. 2022. Many-body self-interaction and polarons. *Phys. Rev. Lett.* 129: 126401

18. Perdew JP, Zunger A. 1981. Self-interaction correction to density functional approximations for many-electron systems. *Phys. Rev. B* 45:5048-5079

19. Shahi C, Bhattarai P, Wagle K, Santra B, Schwalbe S, Hahn T, Kortus J, Jackson KA, Yamamoto Y, Baruah T, Zope R, Perdew JP. 2019.

Stretched or noded orbital densities and self-interaction correction in density functional theory. *J. Chem. Phys.* 150:174102

20. Booth GH, Cleland D, Thom AJW, Alavi A. 2011. Breaking the carbon dimer: The challenges of multiple bond dissociation with full , interaction with quantum Monte Carlo methods. *J. Chem. Phys.* 135:084104

21. Moreira IPR, Illas F, Martin RL. 2002. Effect of Fock exchange on the electronic structure and magnetic coupling in NiO. *Phys. Rev.* B 65: 155103

22. Ellis JK, Martin RL, Scuseria, GE. 2013. On pair functions and strong correlations. *J. Chem. Theory Comput.* 9:2857-2869

23. Khamoshi A, Chen G, Evangelista F, Scuseria GE. 2022. AGP-based unitary coupled-cluster theory for quantum computers. *Quantum Science and Technology*, accepted.

24. Perdew JP, Ernzerhof M, Burke K, Savin A. 1997. On-top pair density interpretation of spin density functional theory, with applications to magnetism. *Int. J. Quantum Chem.* 61:197-205

25. Gunnarsson O, Lundqvist BI. 1976. Exchange and correlation in atoms, molecules, and solids by the spin-density functional formalism. *Phys. Rev. B* 13:4274-4298

26. Su NQ, Li C, Yang W. 2018. Describing strong correlation with fractional-spin correction in density functional theory. *Proc. Nat. Acad. Sci. USA* 115(39): 9678-9683

27. Kirkpatrick J, McMorrow B, Turban DHP, Gaunt AL, Spencer JS, Matthews AGDG, Obika A, Thiry L, Fortunato M, Pfau D, Castellanos LR, Petersen S, Nelson AWR, Kohli P, Mori-Sánchez P, Hassabis D, Cohen AJ. 2021. Pushing the frontiers of density functional theory by solving the fractional electron problem. *Science* 374:1385-1389

28. Zunger A. 2022. Bridging the gap between density functional theory and quantum materials. *Nature Computational Science* 2:529-532

29. Anderson PW. 1972. More is different: Broken symmetry and the hierarchical structure of science. *Science* 177:393-396

30. Perdew JP, Ruzsinszky A, Sun J, Nepal NK, and Kaplan AD. 2021. Interpretations of ground-state symmetry breaking and strong correlation in wavefunction and density functional theories. *Proceedings of the National Academy of Sciences USA* 118:e2017850118

31. Chowdhury STuR, Perdew JP. 2021. Spherical vs. non-spherical and symmetry-preserving vs. symmetry-breaking densities in density functional theory. *J. Chem. Phys.* 155(23):234110

32. Bylaska EJ, Tsemekhman K, Govind N, Valiev M. 2011. Large-scale plane-wave-based density functional theory: Formalism, parallelization, and applications. In *Computational Methods for Large Systems* 77:116.

33. Aprà E, Bylaska EJ, De Jong WA, Govind N, Kowalski K, Straatsma TP, Valiev M, van Dam HJJ, Alexeev Y, Anchell J, Anisimov V, Aquino FW, Atta-Fynn R, Autschbach J, Bauman NP, Becca JC, Bernholdt DE, Bhaskaran-Nair K, Bogatko S, Borowski P, Boschen J, Brabec J, Bruner A, Cauët E, Chen Y, Chuev GN, Cramer CJ, Daily J, Deegan MJO, Dunning TH, Dupuis M, Dyall KG, Fann GI, Fischer SA, Fonari A, Früchtl H, Gagliardi L, Garza J, Gawande N, Ghosh S, Glaesemann K, Götz AW, Hammond J, Helms V, Hermes ED, Hirao K, Hirata S, Jacquelin M, Jensen L, Johnson BG, Jónsson H, Kendall RA, Klemm M, Kobayashi R, Konkov V, Krishnamoorthy S, Krishnan M, Lin Z, Lins RD, Littlefield RJ, Logsdail AJ, Lopata K, Ma W, Marenich AV, Martin del Campo J, Mejia-Rodriguez D, Moore JE, Mullin JM, Nakajima T, Nascimento DR, Nichols JA, Nichols PJ, Nieplocha J, Otero-de-la-Roza A, Palmer B, Panyala A, Pirojsirikul T, Peng B, Peverati R, Pittner J, Pollack L, Richard RM, Sadayappan P, Schatz GC, Shelton WA, Silverstein DW, Smith DMA, Soares TA, Song D, Swart M, Taylor HL, Thomas GS, Tipparaju V, Truhlar DG, Tsemekhman K, Van Voorhis T, Vázquez-Mayagoitia, Á, Verma P, Villa O, Vishnu A, Vogiatzis KD, Wang D, Weare JH, Williamson MJ, Windus TL, Woliński K, Wong AT, Wu Q, Yang C, Yu Q, Zacharias M, Zhang Z, Zhao Y, Harrison RJ. 2020. NWChem: Past, present, and future. *J. Chem. Phys.* 152(18):184102.

34. Valiev M, Bylaska EJ, Govind N, Kowalski K, Straatsma TP, van Dam HJJ, Wang D, Nieplocha J, Aprà E, Windus TL, De Jong WA. 2010. NWChem: A comprehensive and scalable open-source solution for large scale molecular simulations. *Comput. Phys. Commun.* 181(9):1477-1489.

35. Bylaska EJ, Song D, Ilton ES, O'Leary S, Torralba-Sánchez TL, Tratnyek PG. 2021. Building toward the future in chemical and

materials simulation with accessible and intelligently designed web applications. In *Annu. Rep. Comput. Chem.* 17:163-208 (Elsevier)

36. Hamann DR. 1989. Generalized norm-conserving pseudopotentials. *Phys. Rev. B* 40(5):2980-2987

37. Kleinman L, Bylander DM. 1982. Efficacious form for model pseudopotentials. *Phys. Rev. Lett.* 48(20):1425-1428

38. Bylaska EJ, Taylor PR, Kawai R, Weare JH. 1996. LDA predictions for C_{20} isomerization: Neutral and charged species. *J. Phys. Chem.* 100: 6966-6972

39. Bylaska EJ, Valiev M, Kawai R, Weare JH. 2002. Parallel implementation of the projector augmented plane wave method for charged systems. *Comput. Phys. Commun.* 143(1):11-28

40. Dunlap BI. 1983. Basis set effects on spectroscopic constants for C_2 and Si_2 and the symmetry dilemma in the *$X\alpha$* model. *J. Chem. Phys.* 78:4997.

41. Perdew JP, Chevary JA, Vosko SH, Jackson KA, Pederson MR, Singh DJ, Fiolhais C. 1992. Atoms, molecules, solids, and surfaces: Applications of the generalized gradient approximation for exchange and correlation. *Phys. Rev. B* 46:6671-6687

42. Langreth DC, Perdew JP. 1975. The exchange-correlation energy of a metallic surface. *Solid State Commun.* 17:1425-1429

Table I. Atomization energy (eV) of singlet C_2 at its equilibrium bond length from several nonempirical density functionals, calculated without and with spin-symmetry breaking (SB) in the molecule. All the equilibrium bond distances were obtained by DFT geometry optimization (R_{eq} = 1.24 Å from restricted LSDA, 1.27 Å from unrestricted LSDA, 1.25 Å from restricted PBE GGA, 1.29 Å from unrestricted PBE GGA, 1.23 Å from restricted SCAN meta-GGA and 1.27 Å from unrestricted SCAN meta-GGA). The reference value is the FCIQMC value from Ref. 20, which found R_{eq} = 1.24 Å. (1 hartree = 27.21 eV = 627.5 kcal/mol)

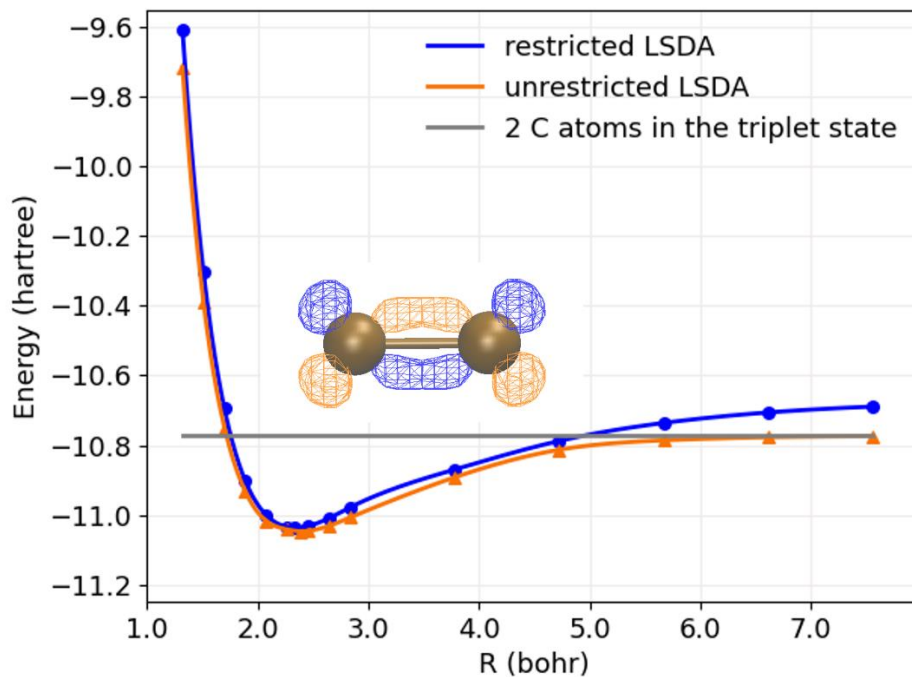| Functional	without SB	with SB	difference
LSDA	7.19	7.47	0.28
PBE GGA	6.03	6.75	0.72
SCAN meta-GGA	4.76	6.19	1.43
reference		6.22	

Fig. 1. LSDA binding energy curve for singlet C_2. Pseudopotential energy in hartree vs. bond length in bohr. Blue: without symmetry breaking in the molecule. Orange: with spin-symmetry breaking in the molecule. The inset shows +0.05 (orange) and -0.05 au (blue) contour surfaces of $n_\uparrow - n_\downarrow$ for the symmetry-broken solution at the equilibrium bond length $R_{eq} = 2.39$ bohr (1.27 Å).
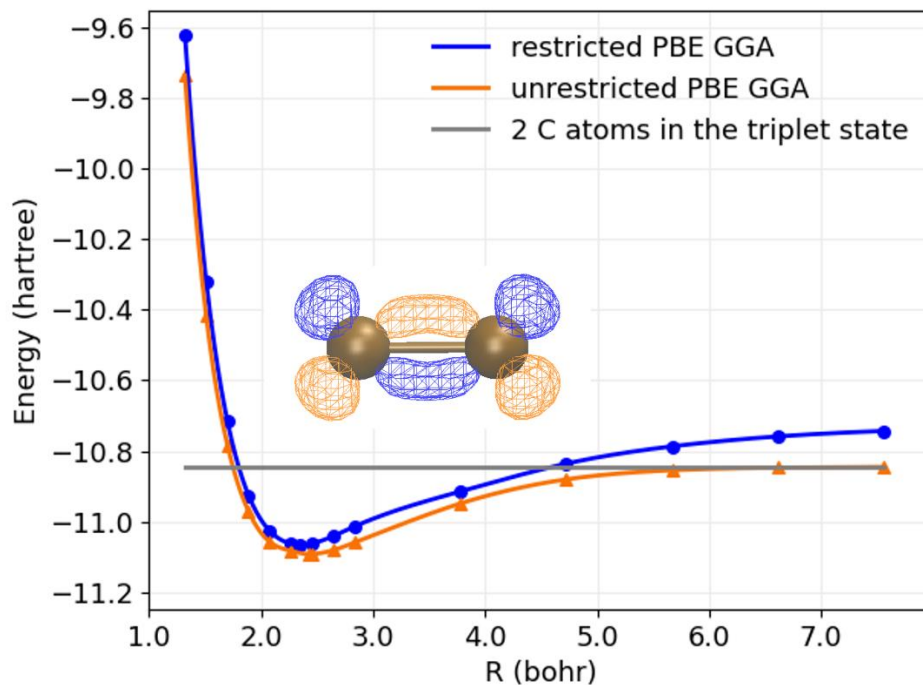
Fig. 2. PBE GGA binding energy curve for singlet C_2. Pseudopotential energy in hartree vs. bond length in bohr. Blue: without symmetry breaking in the molecule. Orange: with spin-symmetry breaking in the molecule. The inset shows +0.05 (orange) and -0.05 au (blue) contour surfaces of $n_\uparrow - n_\downarrow$ at the equilibrium bond length R_{eq} = 2.43 bohr (1.29 Å).
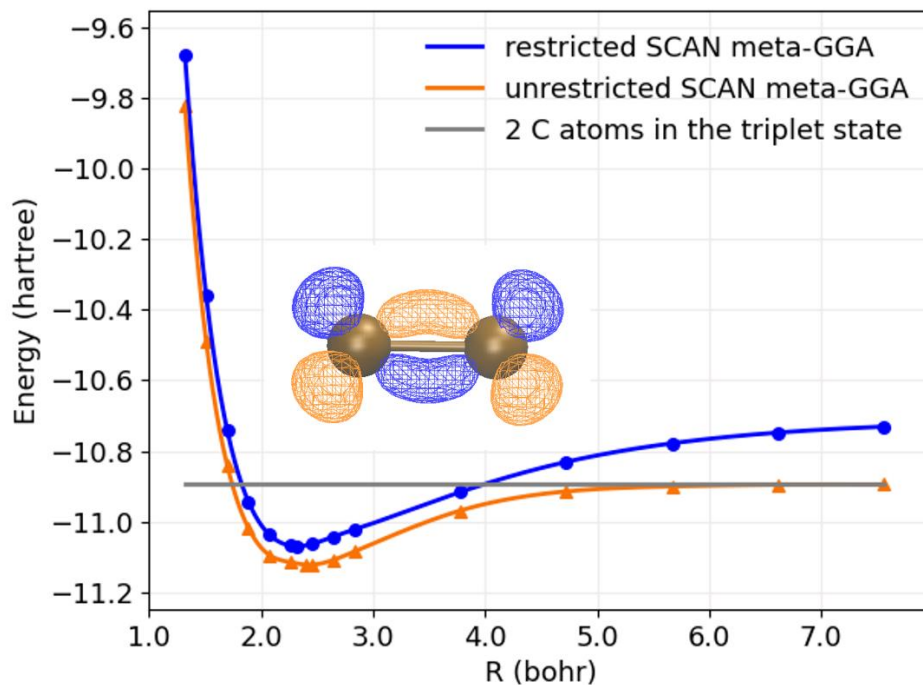
Fig. 3. SCAN meta-GGA binding energy curve for singlet C_2. Pseudopotential energy in hartree vs. bond length in bohr. Blue: without symmetry breaking in the molecule. Orange: with spin-symmetry breaking in the molecule. The inset shows +0.05 (orange) and -0.05 au (blue) contour surfaces of $n_\uparrow - n_\downarrow$ at the equilibrium bond length $R_{eq} = 2.41$ bohr (1.27 Å).